

UC Berkeley

UC Berkeley Previously Published Works

Title

Mineral protection of soil carbon counteracted by root exudates

Permalink

<https://escholarship.org/uc/item/9g04p5md>

Journal

Nature Climate Change, 5(6)

ISSN

1758-678X

Authors

Keiluweit, Marco
Bougoure, Jeremy J
Nico, Peter S
[et al.](#)

Publication Date

2015-06-01

DOI

10.1038/nclimate2580

Peer reviewed

Mineral protection of soil carbon counteracted by root exudates

Marco Keiluweit^{1,2}, Jeremy J. Bougoure, Peter S. Nico, Jennifer Pett-Ridge, Peter K. Weber & Markus Kleber

¹Department of Crop and Soil Science, Oregon State University, ALS Building 3017, Corvallis, Oregon 97331, USA

²Chemical Sciences Division, Lawrence Livermore National Laboratory, 7000 East Avenue, L-231, Livermore, California 94550, USA

Published 30 March 2015

DOI: <https://doi.org/10.1038/nclimate2580>

Abstract

Multiple lines of existing evidence suggest that climate change enhances root exudation of organic compounds into soils. Recent experimental studies show that increased exudate inputs may cause a net loss of soil carbon. This stimulation of microbial carbon mineralization ('priming') is commonly rationalized by the assumption that exudates provide a readily bioavailable supply of energy for the decomposition of native soil carbon (co-metabolism). Here we show that an alternate mechanism can cause carbon loss of equal or greater magnitude. We find that a common root exudate, oxalic acid, promotes carbon loss by liberating organic compounds from protective associations with minerals. By enhancing microbial access to previously mineral-protected compounds, this indirect mechanism accelerated carbon loss more than simply increasing the supply of energetically more favourable substrates. Our results provide insights into the coupled biotic–abiotic mechanisms underlying the 'priming' phenomenon and challenge the assumption that mineral-associated carbon is protected from microbial cycling over millennial timescales.

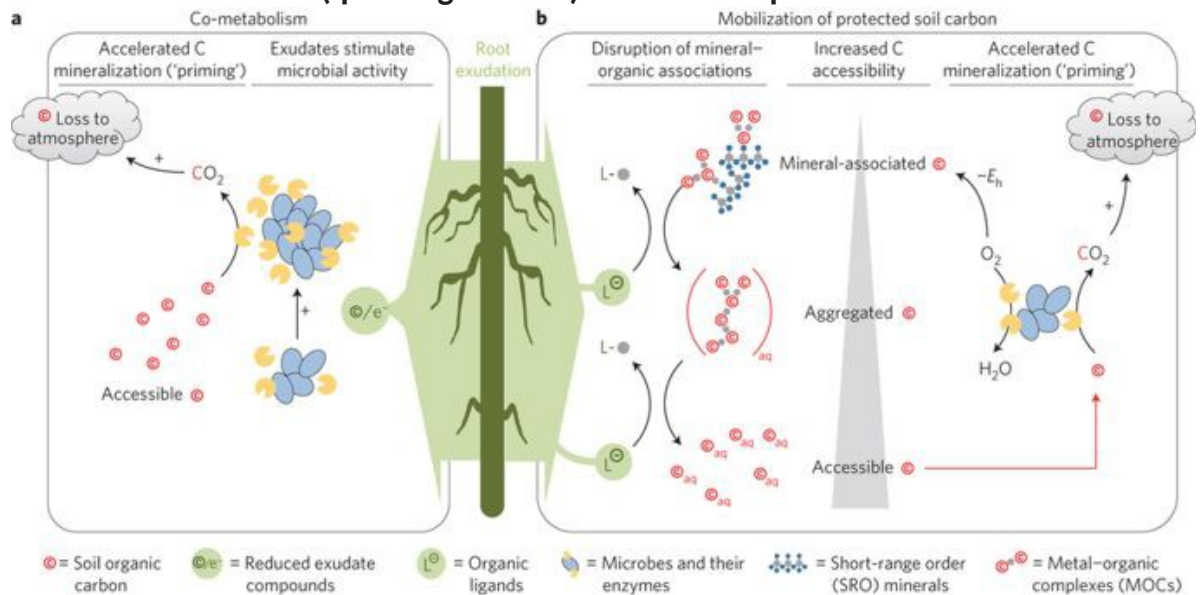
Main

Plants direct between 40–60% of photosynthetically fixed carbon (C) to roots and associated microorganisms via sloughed-off root cells, tissues, mucilage and a variety of exuded organic compounds^{1,2}. Elevated CO₂ concentrations in the atmosphere are projected to increase the quantity^{3,4} and alter the composition^{5,6} of root exudates released into the soil. It seems less clear to what extent changing inputs will cause a net loss of native (or 'old') organic C (ref. [7](#)). A better understanding of the mechanism underlying soil C loss is pivotal in predicting how the large soil C stocks may respond to global change.

Exudate-induced soil C loss is commonly attributed to a 'priming effect'—that is, a short-term increase in microbial mineralization of native soil C as a result of fresh carbon inputs to the soil⁸. Although the process of 'priming' has received great attention in ecosystem sciences in recent years^{8,9}, our knowledge of the underlying mechanism is limited. It is often supposed that bioavailable exudate compounds induce greater microbial activity and enzyme production because they serve as 'co-metabolites'^{8,10}. Co-metabolism is defined as the mineralization of a non-growth substrate (for example, certain forms of native soil organic C) during growth of a microorganism on a bioavailable carbon and energy source (for example, exudate compounds)¹¹. This mechanism is

often invoked to increase the physiological potential of decomposers for the mineralization of native soil C (refs 8, 10) (Fig. 1a). However, as noted by Kuzyakov and co-workers¹², direct experimental evidence in support of this mechanism is scarce because most studies have aimed at identifying ‘priming effects’ rather than the underlying mechanism.

Figure 1: Proposed mechanisms for the exudate-induced acceleration of the microbial mineralization of native carbon (‘priming effects’) in the rhizosphere.



[Full size image](#)

a, The traditional view is that reduced exudate compounds (for example, simple sugars) stimulate microbial growth and activity via co-metabolism, and so increase the overall physiological potential of the decomposer community for carbon mineralization. Other factors such as the increased microbial demand for nitrogen or successional shifts in the community structure may also contribute to increased mineralization rates^{8,12}. **b**, The alternative mechanism proposed here takes into account that large quantities of soil C are inaccessible to microbes owing to associations with mineral phases. Root exudates that can act as ligands (for example, organic acids) effectively liberate C through complexation and dissolution reactions with protective mineral phases, thereby promoting its accessibility to microbes and accelerating its loss from the system through microbial mineralization. Microbial O₂ consumption may further increase the accessibility of protected C by lowering the redox potential, E_h , and promoting reductive dissolution of SRO minerals.

Previous attempts to describe the mechanism(s) underlying ‘priming effects’ have focused almost exclusively on biological phenomena. That approach, however, results in a conceptual conundrum: how can observed ‘priming effects’ be explained solely by co-metabolism if microbial access to substrate C is notoriously limited in most soils? In mineral soil, the majority of organic compounds is intimately associated with reactive mineral phases^{13,14}. Metal-organic complex (MOC) and short-range order (SRO) phases bind organic compounds through their large surface area and various bonding sites^{15,16}. Such mineral-organic associations limit microbial and enzymatic access¹⁷ and are quantitatively the most important mechanism protecting C from microbial use for centuries or millennia¹⁸. Rasmussen *et al.*¹⁹ showed that the magnitude of the ‘priming effect’ is at least partly

controlled by the presence of reactive mineral phases. Recent conceptual frameworks^{20,21} and numerical models²² therefore argue that C mineralization rates are generally enhanced by mechanisms that facilitate the release of mineral-protected C into more accessible pools.

Here we tested whether the acceleration of carbon mineralization in the rhizosphere (that is, the priming effect) is promoted by the exudates' ability to liberate C from protective mineral-organic associations, thereby increasing microbial access. In a well-controlled system, we investigated the effects of the two most abundant exudate classes—organic acids and simple sugars^{23,24}. We hypothesized that direct dissolution of protective mineral phases would be promoted by oxalic acid ([Fig. 1b](#)). Oxalic acid—an organic acid produced by roots, root-associated fungi and bacteria—is routinely found among the most abundant compounds in rhizosphere pore water^{23,24}. Oxalic acid has strong metal-complexing abilities but is of limited bioenergetic use to microbes. In contrast, we expected bioenergetically more favourable sugars such as glucose to act as a co-metabolite and stimulate microbial mineralization of native soil C ([Fig. 1a](#)). A third common exudate, acetic acid, was expected to have an intermediate response, as it is less easily metabolized than glucose and has a lower complexing capacity than oxalic acid ([Table 1](#)).

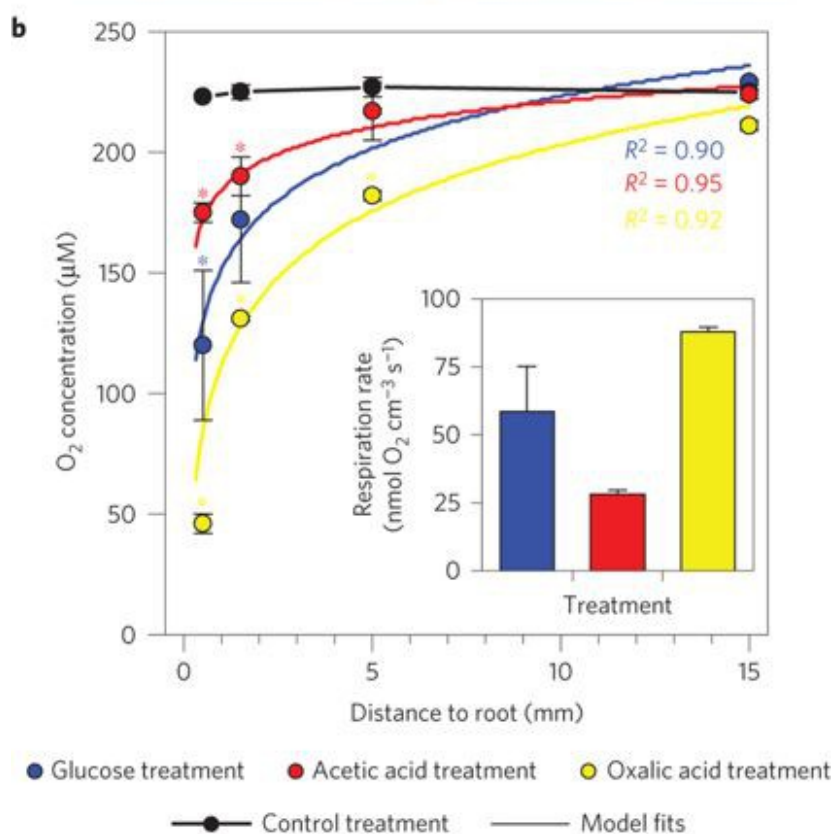
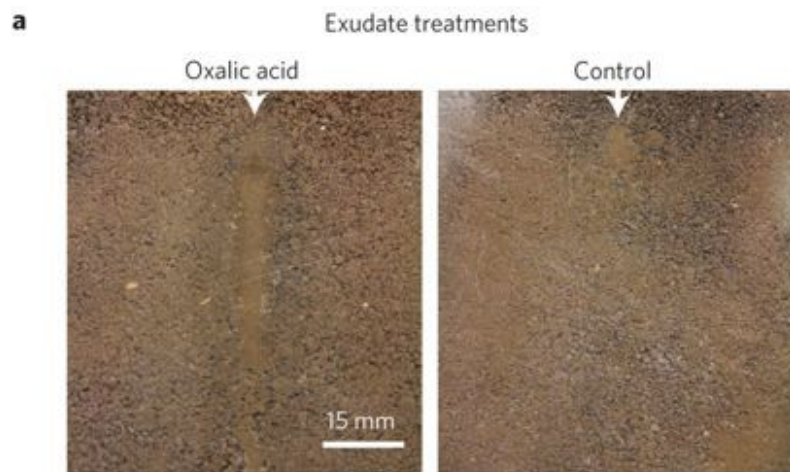
Table 1: Exudate properties and their predicted and measured effect on microbial carbon-use efficiency (CUE) and biochemical oxygen demand (BOD).

[Full size table](#)

Recreating a rhizosphere environment

We tested these hypotheses by delivering a continuous supply of individual exudate solutions through an artificial root (length = 10 cm, diameter = 2.5 mm) into unperturbed soil, recreating a rhizosphere environment ([Supplementary Fig. 1](#)). Exudates were supplied to a grassland soil ([Supplementary Table 1](#)) at root surface-normalized rates mimicking natural exudation rates of root tips ($15 \mu\text{mol C cm}^{-2} \text{ d}^{-1}$; refs [25](#), [26](#)). For comparison, selected analyses were replicated with a forest soil. To distinguish exudate C from native soil C, individual exudate solutions were isotopically labelled with ^{13}C ($\delta^{13}\text{C} = 8,800\text{‰}$). Exudate solutions or an inorganic nutrient solution (control) were provided over an incubation period of 35 days to replicate a burst in root growth at the onset of the growing season when the highest exudation rates are expected²⁶. Compared to the control, all three exudate compounds induced visible physical gradients surrounding the artificial root after 7–10 days, which remained stable until the end of the experiment. In the oxalic acid treatment, these pronounced effects developed around the entire root and extended up to 5–10 mm into the soil ([Fig. 2a](#)), but in soils receiving glucose and acetic acid additions were limited to small patches around the root.

Figure 2: Exudate effects on artificial rhizosphere soil.



[Full size image](#)

a, Photographs of the rhizosphere effect caused by oxalic acid addition and the control for comparison. White arrows indicate positions of the artificial root providing exudate solutions. **b**, O₂ concentrations as a function of distance to the root for the different exudate treatments. Points represent mean ± s.e.m. ($n = 2$). Asterisks denote locations with mean O₂ concentrations significantly lower than the control (one-way ANOVA, Tukey's ad hoc HSD test, $p < 0.05$). Solid lines represent model fits used to calculate microbial respiration based on Fick's first law of diffusion⁵³. The inset shows volume-specific respiration rates in the rhizosphere for each exudate treatment. See [Supplementary Information](#) for details on fitting parameters and rate calculations.

If root exudates were to accelerate the microbial mineralization of soil C (that is, cause 'priming effects') primarily because they serve as a co-metabolite (that is, provide easily assimilable C and energy; [Fig. 1a](#)), one would expect energetically favourable glucose to cause a greater 'priming effect' than less favourable substrates such as oxalic acid ([Table 1](#)). However, we found that oxalic acid additions led to greater microbial respiration, community shifts to fast growing, rapidly C-mineralizing microbial taxa, and loss of total soil C relative to the other treatments. This accelerated microbial C mineralization caused by oxalic acid exudates coincided with the disruption of mineral-organic associations and increases in C accessibility in the pore water. The following describes evidence that this 'priming effect' is at least in part caused by the exudates' ability to enhance microbial access to previously protected soil C ([Fig. 1b](#)).

Oxalic acid accelerated soil carbon mineralization

To determine the effect of root exudates on microbial respiration rates in rhizosphere microsites, we used microsensors to record O₂ profiles in the soil surrounding the root ([Fig. 2b](#)). These profiles showed that addition of oxalic acid significantly depleted O₂ availability up to 5 mm into the surrounding soil ($p < 0.05$; [Fig. 2b](#)), whereas the effects of glucose and acetic acid additions were restricted to the first 1.5 mm. Across the entire rhizosphere zone (0–15 mm), microbial respiration rates followed a consistent pattern: oxalic acid > glucose > acetic acid ([Fig. 2b](#), inset). To test whether this was a response specific to the grassland soil (silt-loam), we repeated the experiment with a forest soil (clay-loam) differing in texture and mineralogy ([Supplementary Table 1](#)) and observed the same result ([Supplementary Fig. 1](#)). Overall, microbial respiration in the oxalic acid treatment exceeded that of glucose by factors of ~1.6 (silt-loam) and ~2.8 (clay; [Table 1](#)).

We compared the stoichiometry of microbial carbon-use efficiency (CUE) and biochemical oxygen demand (BOD) of oxalic acid versus glucose mineralization pathways and found that oxalic acid addition accelerated the mineralization of native soil C more than glucose addition. Reported CUEs (the ratio of C assimilated into new biomass relative to the amount of C used in cellular respiration) for oxalic acid (5–25%) and glucose (40–70%) in soils^{27,28,29} indicate that the fraction of oxalic acid C released as CO₂ (75–95%) is about twice that of glucose C (30–60%). Mineralization (that is, complete oxidation) of oxalic acid to CO₂ requires 0.25 moles of O₂ per unit C compared to 1 mole of O₂ per unit C for glucose ([Table 1](#)). The BOD expected for the mineralization of each substrate is equal to:

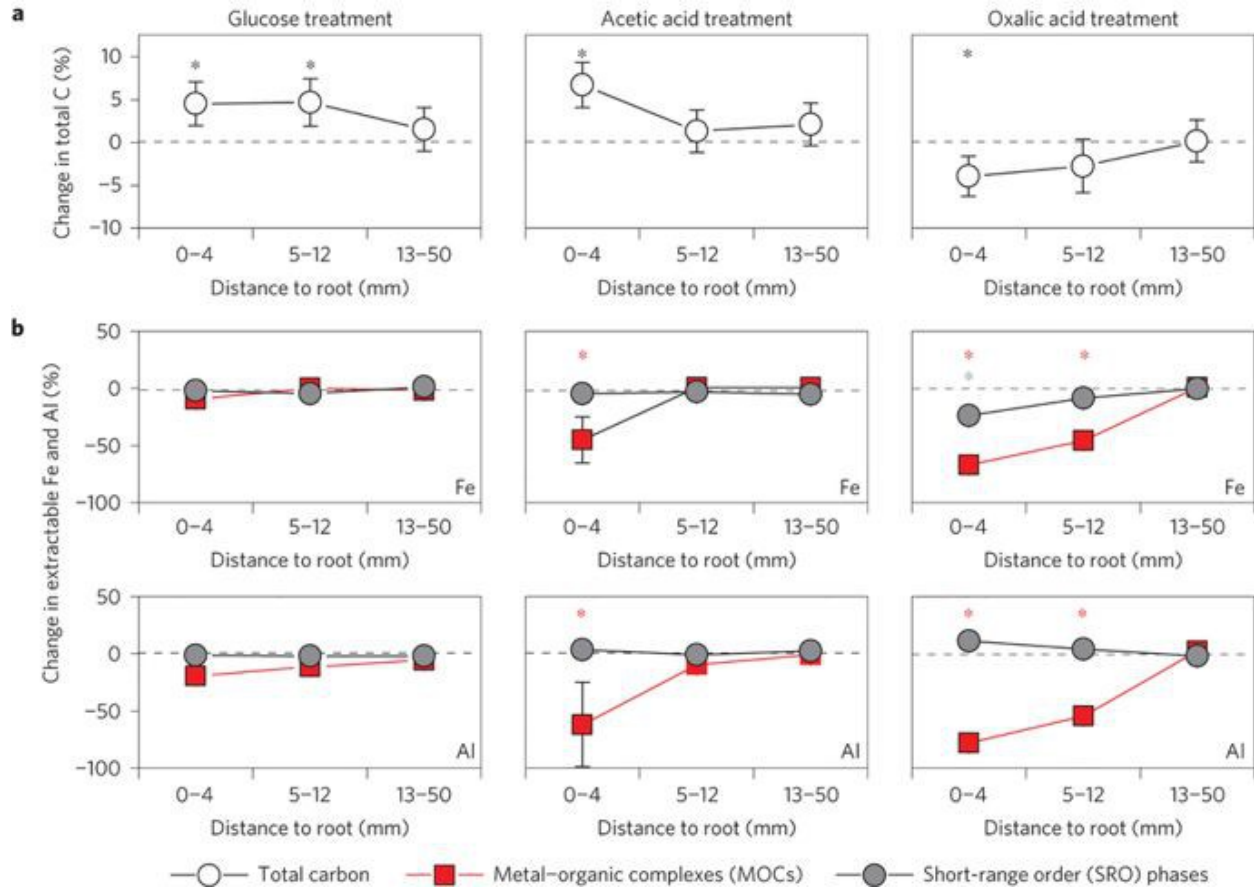
$$\text{Expected BOD} = (1 - \text{CUE}) \times \text{stoichiometric BOD}$$

The CUE and stoichiometric BOD values used are shown in [Table 1](#). These calculations demonstrate that the BOD expected for microbial mineralization of oxalic acid should be only half the value associated with glucose mineralization ([Table 1](#)). Because our measured respiration rates show the opposite trend, we conclude that mineralization of other, more reduced (non-exudate) soil C must have accounted for at least 50% of the respiration observed in the oxalate treatment.

In line with accelerated mineralization of native soil C, soils receiving oxalic acid additions experienced a net C loss in the zone closest to the root ($p < 0.05$; [Fig. 3a](#)). In contrast, addition of

the energetically more favourable substrates glucose and acetic acid resulted in a pronounced increase in total soil C content (Fig. 3a). This net C accumulation, possibly due to an increase in microbial biomass C caused by microbial assimilation of these exudates, was not counterbalanced by concurrent increases in the mineralization of native C.

Figure 3: Exudate-induced effects on total soil C and protective mineral phases.



[Full size image](#)

a, Relative changes in total soil C. **b**, Fe and Al bound in metal-organic complexes (MOCs) and short-range order (SRO) phases presented as a function of distance to the root. Treatment effects were calculated as the percentage difference between concentrations in treatment and control samples for each distance. Positive values indicate a treatment-induced pool increase, whereas negative values indicate a pool decrease. Asterisks denote pool sizes significantly different from the control (one-way ANOVA, Tukey's ad hoc HSD, $p < 0.05$). Values are shown as means \pm s.e.m. ($n = 2$). Data shown for silt-loam grassland soils only. Changes in metal pools of the clay-rich forest soil can be found in [Supplementary Fig. 6](#).

Pronounced compositional changes in microbial community structure also reflect greater carbon mineralization activity in soil receiving oxalic acid ([Supplementary Fig. 3a](#)). Near the root (0-4 mm), oxalic acid additions significantly increased the relative abundance of *Bacteroides* and *Proteobacteria* and reduced that of *Acidobacteria*, *Firmicutes* and *Verrucomicrobia* ($p < 0.05$; [Supplementary Fig. 3b](#)). Microbial communities in soils amended with acetic acid soils shifted in a similar but less pronounced manner relative to soils treated with oxalic acid; glucose had very little effect. Taxa from the *Bacteroidetes* and *Proteobacteria* phyla that were strongly promoted by the

oxalic acid treatment are often characterized as copiotrophs, and positively correlated with increased C bioavailability and mineralization rates^{30,31}.

Excess dissolved CO₂ measured in the pore water provides further evidence for accelerated C mineralization in the oxalic acid treatment. Measured immediately after harvest, the pH of soil close to the root was 1.5 and 0.7 units higher in oxalic and acetic acid treatments, respectively, whereas glucose lowered the pH by 0.5 units ([Supplementary Table 6](#)). This increased proton consumption can be attributed to one or a combination of factors, all of which are linked to increased microbial activity: microbial decarboxylation³², mineral dissolution reactions³³, dissimilatory metal reduction³⁴ and/or denitrification³⁵. More importantly, however, we observed further pH increases in the oxalic acid treatment when samples were allowed to equilibrate with the atmosphere. This observation suggests that removal of excess dissolved CO₂, produced by microbial mineralization over the course of the incubation, diminished the buffering capacity of the soil.

In summary, we find that oxalic acid additions accelerate microbial C mineralization and lead to a significant loss of native C (~4%), consistent with previous observations of strong 'priming effects' induced by oxalic acid^{36,37}.

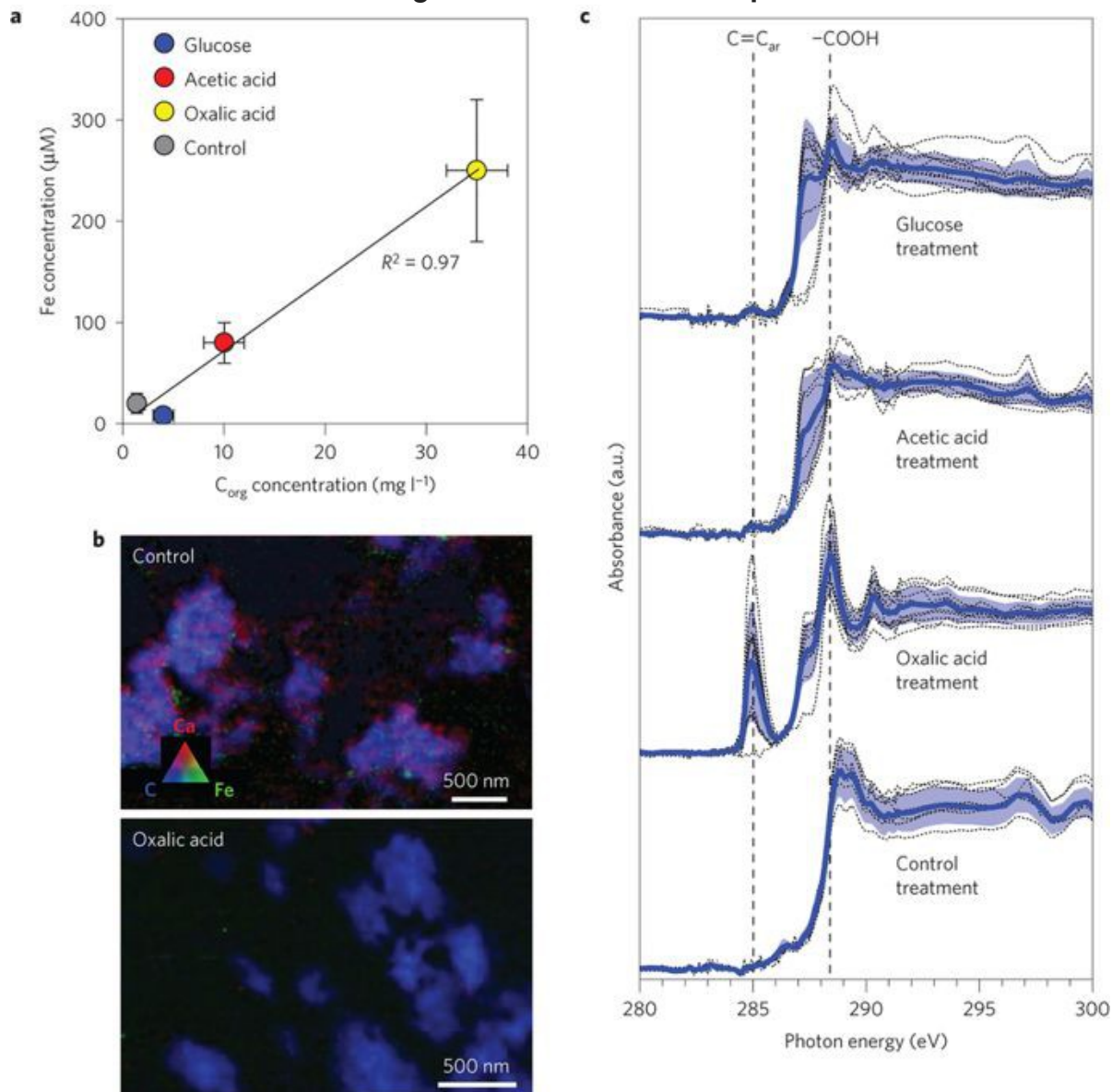
Spectroscopic insights into the 'priming' mechanism

To test whether disruptions of protective mineral–organic associations are responsible for the 'priming effect' we observed, sequential extractions targeting MOC and SRO phases were performed ([Fig. 3b](#)). Compared to the control, oxalic acid addition significantly decreased concentrations of Fe and Al phases up to 12 mm into the soil ($p < 0.05$). Specifically, Fe and Al in MOCs decreased with increasing proximity to the root, paralleled by a notable decline of Fe in SRO phases. Acetic acid exudates also significantly reduced the amount of Fe and Al in MOCs in the zone closest to the root ($p < 0.05$), whereas glucose showed no measurable effect. There were no significant responses of more crystalline pools to the exudate treatments. Complementary batch experiments showed that oxalic acid caused greater mobilization of Fe and Al after a short incubation of 1 h than after a prolonged incubation period (48 h; [Supplementary Table 10](#)); glucose showed no such effect. We infer that, in our system, physiological levels of oxalic acid disrupt mineral–organic associations via an immediate, abiotic mechanism rather than slower, microbially mediated processes. This mechanism is more effective for mineral–organic associations formed by amorphous MOCs than for such that are composed of more crystalline SRO phases—a result consistent with observations of stronger 'priming effects' (that is, accelerated mineralization of native soil C) in soils dominated by amorphous MOCs than in soils characterized by more crystalline metal oxides phases¹⁹.

We further examined the concentration and speciation of pore water C and metals as a test for the liberation of mineral-bound organic C ([Supplementary Table 6](#)). In the near-root zone (0–4 mm), oxalic acid addition increased pore water C concentrations by a factor of ~8 compared to the control, whereas acetic acid and glucose additions affected C concentrations by factors of only ~2.5 and ~1, respectively. This increase in dissolved C in the pore water correlated with increases in

dissolved Fe ($R^2 = 0.98$) and Al ($R^2 = 0.95$; [Fig. 4a](#) and [Supplementary Table 6](#)). The bulk chemical composition of organic C in the pore water was determined by laser desorption post ionization mass spectrometry (LDPI-MS), a method that is particularly sensitive for lignin-derived compounds³⁸. Mass spectra of pore water from the oxalic acid treatment showed a notably greater abundance of high mass-to-charge peaks ($m/z = 250$ to 500) relative to the other treatments ([Supplementary Fig. 4](#)). These mass peaks can be attributed to aromatic dimers based on the relatively low ionization energy of aromatic compounds³⁹ and peak patterns resembling those of lignin in soils³⁸. These results support the hypothesis that oxalic acid addition chemically disrupted MOCs and SRO mineral phases in the rhizosphere ([Fig. 3b](#)) and increased pore water concentrations of C and metals more than either glucose or acetic acid ([Fig. 4a](#)). Oxalic acid additions seem to increase microbial access to C in the pore water via this mechanism.

Figure 4: Exudate effect on metal-organic associations in the pore water.



a, C mobilization into the pore water in relation to dissolved Fe concentrations. b, Ca and Fe associated with dissolved organic C collected from control and oxalic acid treatments. Maps are generated as difference maps of two image scans collected above and below the respective absorption edge energies. c, Carbon K-edge NEXAFS spectra of pore water C. Spectra of discrete regions of interest are shown as dotted lines, with the blue lines and shaded areas representing mean and standard deviation, respectively. The numbers of regions analysed for glucose, acetic acid and oxalic acid were 8, 9 and 10, respectively, with 9 regions for the control. Data shown for silt-loam grassland soils only. Carbon NEXAFS spectra for clay-rich forest soil ([Supplementary Fig. 5](#)) and details on the STXM maps can be found in the [Supplementary Information](#).

To gain more detailed insights into the mechanisms of C mobilization, the chemical form of pore water C and its association with inorganic constituents was determined using nanoscale secondary ion mass spectrometry (NanoSIMS) and scanning transmission X-ray microscope/near edge X-ray absorption fine structure (STXM/NEXAFS) imaging. NanoSIMS analysis of organic C in the pore water showed that only a small fraction (<2.5%) was derived from ¹³C-labelled exudates ([Supplementary Table 9](#)). This confirms that exudates are rapidly removed from solution by microbial processing and/or adsorption to minerals⁴⁰, and that dissolved compounds remaining in the pore water are predominantly derived from native soil C. STXM revealed that organic compounds isolated from the oxalic acid treatment showed only traces of Ca (Fe was below the detection limit), whereas organic C from the control treatment was associated with considerable amounts of Ca and Fe. Pore water C from the oxalic acid treatment also featured prominent resonances assigned to aromatic ($1s\text{-}\pi^*$ transitions of conjugated C=C) and carboxylic moieties ($1\text{-}\pi^*$ transition of COOH) in the corresponding NEXAFS spectra ([Fig. 4c](#)). In contrast, spectra of glucose, acetic acid, and control treatments indicated no aromatic C resonances—a pattern that was confirmed in forest soil subjected to the same treatments ([Supplementary Fig. 5](#)). Lignin-derived aromatic acids are strong metal chelators and are often associated with SRO minerals^{41,42}. Crosslinking between these multivalent cations and carboxylic and phenolic groups facilitates aggregation and precipitation of organic compounds⁴³. Oxalic acid, with its high ligand binding constant ([Table 1](#)), strips cations such as Fe and Ca from metal-organic ligand complexes ([Fig. 4b](#)). In our experiment we observed enhanced solubility of organic compounds, supporting the hypothesis that oxalic acid removed the cations from MOCs. On the basis of our results, we conclude that oxalic acid addition increased pore water concentrations of aromatic and carboxylic C ([Fig. 4c](#)) associated with lignin-derived dimers ([Supplementary Fig. 4](#)). Low concentrations of oxalic acid released into the rhizosphere suffice to remobilize such compounds and enhance microbial access.

Implications for terrestrial carbon cycling

As detailed above, we expected that an energetically more favourable root exudate such as glucose should cause a greater 'priming effect' than a less attractive one such as oxalic acid ([Fig. 1a](#)). However, the inverse was observed: by improving the accessibility of C previously protected in mineral-organic associations, oxalic acid induced a much stronger 'priming effect' than glucose and acetic acid. Rather than via co-metabolism, organic ligands with metal-complexing abilities accelerate microbial mineralization of C in the rhizosphere via an indirect, multipart mechanism

([Fig. 1b](#)). Organic ligands released into the rhizosphere (i) mobilize mineral-bound C through complexation and dissolution of SRO phases and/or (ii) solubilize organic compounds through the removal of crosslinking metal cations from MOCs. Release from SRO or MOC phases promotes the accessibility of organic compounds to microbes. Increased microbial access subsequently (iii) stimulates microbial mineralization and shifts the community structure towards phyla adapted to soil environments with greater accessibility of C. On the basis of these results, we conclude that 'priming effects' are not a purely biotic phenomenon and should be viewed as the sum of direct biotic co-metabolic ([Fig. 1a](#)) and indirect C mobilization ([Fig. 1b](#)) mechanisms. We suggest that future investigations into the causes of 'priming effects' consider both mechanisms simultaneously and focus on quantifying their relative contributions in different soil ecosystems.

In our study, oxalic acid disrupted mineral-organic associations in both grassland and forest soils. This observation is consistent with root-induced weathering of protective mineral phases during periods of rapid root growth in arable [44](#) and forest soils [45](#), and highlights the general nature of the proposed mechanism. To estimate the importance of the proposed mechanism at the ecosystem-scale, we calculated the potential C loss that may be attributed to this mobilization mechanism in a forest ecosystem. The oxalic acid treatment resulted in an overall C loss of $\sim 4\%$ over our experimental period. If we assume that the total amount of exudate C released into the soil in our experiments is comparable to that released over the course of an annual burst of root growth in times of high primary productivity [26](#), and organic acids comprise up to $\sim 25\%$ of the mixture of compounds exuded over that time frame [24](#), the annual soil C loss is estimated to be $\sim 1\% \text{ C yr}^{-1}$. By comparison, Richter *et al.* [46](#) found that soil C in deep mineral horizons, where C accessibility is probably low owing to mineral-organic associations, is rapidly mineralized on reforestation and expansion of the rooting zone. In that study, the average loss over four decades of reforestation was approximately $1.08\% \text{ C yr}^{-1}$ —a rate strikingly close to the value in our experiment. Although simple, our calculation highlights the potential impact of the proposed 'priming' mechanism on mineral-protected C at an ecosystem level.

Conceptual frameworks of soil organic matter stabilization have long considered C in mineral-organic associations permanently inaccessible to microbes, and thus protected from loss processes for millennia or longer [13-14-18](#). But this paradigm is shifting, and many now recognize that any natural organic compound can be decomposed when the required resources are available to the decomposer community [21](#). Here we demonstrate a climate-dependent 'priming' mechanism where plant exudates counteract the strong protective effect of mineral-organic associations and facilitate the loss of C from the soil system. This physiological capacity of plant roots to effectively remobilize mineral-associated soil C will have to be factored into next-generation soil C cycling models [22-47](#) if root exudation rates respond to climate change as predicted. Elevated CO_2 concentrations may not only stimulate exudation, they may also alter the composition of exudate compounds released into soil [6-48](#) and so increase metal mobilization in the rooting zone [49](#). If shifts towards greater exudation of reactive weathering agents such as oxalic acid [5](#) can be confirmed, determining how changing exudation patterns impact mineral-protected C should be a high priority for future research.

Methods

Soils were chosen to represent two important biomes, forests and grasslands. Medium-textured silt-loam (Typic Haploxeroll) under cultivation with *Triticum* spp. (Hermiston Agricultural Research & Extension Center) and volcanic-ash clay (Humic Dystrudepts) under old-growth Douglas-fir (H.J. Andrews Experimental Forest, Oregon, USA). At both sites, soil cores and mixed samples of surface horizons characterized by dense root networks were collected and stored at field moisture at 4 °C until further use (see [Supplementary Table 1](#) for soil characteristics and handling).

Incubations were conducted in microcosm systems designed and fabricated to deliver a continuous supply of exudate solution through an artificial root into the soil (see [Supplementary Information](#) for details). Soils were sieved (2 mm), pre-incubated at 75% field capacity for one week, and packed into the frame at field bulk density. The artificial roots were connected to a syringe pump equipped with a multi-syringe feeding system, which provided sterile exudate solutions containing glucose, acetic acid or oxalic acid as well as inorganic nutrients for osmoregulation (330 μM KCl, 70 μM KH_2PO_4 and 70 μM MgSO_4). Concentrations of each exudate solution were normalized on a C-basis and the pump rate was adjusted such that exudates were delivered at a rate of 15 $\mu\text{mol C cm}^{-2} \text{ d}^{-1}$ per microcosm at 1 ml d^{-1} . ^{13}C -labelled substrates (Cambridge Isotope Laboratories) were used to enrich exudate solutions in ^{13}C (final $\delta^{13}\text{C} = 8,800\text{‰}$). Incubations were carried out in the dark for 35 days, with temperature (25 °C) and relative humidity (75%) controlled by an environmental chamber. Two replicate microcosms were assembled for each treatment.

O_2 concentration profiles were measured after the incubation period using Clark-type microsensors (OX-100, Unisense). Microsensors had a 100- μm tip size, a stirring sensitivity of <2%, and a 90% response time of <1 s. Linear calibrations were performed in 0.1 M sodium ascorbate in 0.1 M NaOH (0% O_2 saturation) and air bubbled water (100% O_2 saturation) before and between measurements. The microsensor was mounted on a micromanipulator (MM33-2, Unisense) and connected to a picoamperemeter (PA-2000, Unisense) to collect six replicate measurements at distances of 0.5, 1, 5 and 15 mm from the root in each microcosm (see [Supplementary Information](#) for details).

After the incubation, microcosms were opened in an anaerobic glove box and three zones on both sides of the root (0–4, 5–12 and 13–50 mm from the root) were carefully sampled for metal and DNA/RNA extractions, pH and total C measurements. Metal pools in each zone were determined using a sequential extraction procedure consisting of 0.1 M Na-pyrophosphate at pH 10 for organically complexed pools and 0.2 M ammonium oxalate at pH 3 for short-range order phases. Duplicate extractions were performed under anaerobic conditions in the dark. Elemental analysis of the supernatants was performed on a Perkin Elmer SCIEX Elan DRC II inductively coupled plasma mass spectrometer (ICP-MS). Total RNA/DNA was extracted from 0.25 g soil of each zone using a MoBio PowerSoil RNA Isolation Kit in combination with the PowerSoil DNA Elution Accessory Kit (MoBio Laboratories) following manufacturer's instructions. Duplicate extracts for each sample were prepared for pyrosequencing (see [Supplementary Information](#) for details).

Soil pore water was extracted from the root zone (0–4 mm) using a Whatman Centrex MF Disposable Centrifugal Microfilter, adapting an existing low-pressure centrifugal displacement

technique⁵⁰. In the glove box, a 2 g aliquot of moist soil was transferred to the sample reservoir. Soil pore water was displaced and filtered through pre-rinsed 0.45 µm cellulose acetate membranes into the collection tube by centrifugation at 2,000g for 60 min. Organic C concentrations in the pore water samples were determined by ultraviolet/visible spectrometry (450 nm) and the chemical composition was analysed using laser desorption synchrotron ionization (LDSI). LDSI was performed on a modified time-of-flight secondary ion mass spectrometer (TOF.SIMS V; IonTOF) coupled to a synchrotron vacuum ultraviolet light port at beamline 9.0.2 of the Advanced Light Source (ALS) at the Lawrence Berkeley National Laboratory. For combined imaging analysis of pore water C and associated metals, 1 µl pore water aliquots were dried on Si₃N₄ windows (Silson) in the glove box. STXM/NEXAFS spectromicroscopic analyses were performed at beamline 5.3.2.2 of the ALS (ref. [51](#)). δ¹³C values of pore water C were acquired using high-resolution secondary ion mass spectrometry imaging performed on a NanoSIMS 50 (Cameca) at the Lawrence Livermore National Laboratory. Details on imaging analyses can be obtained in the [Supplementary Information](#). Reported results from statistical tests were obtained with OriginPro (OriginLab), including one-way ANOVA followed by post hoc analysis using Tukey's HSD test ([Figs 2b](#) and [3](#)) and correlation analysis ([Fig. 4a](#)), with a *p*-value of less than 0.05 indicating statistical significance.

Acknowledgements

The authors thank A.L.D. Kilcoyne (ALS beamline 5.3.2.2), S.Y. Liu and M. Ahmed (ALS beamline 9.0.2) for their support. M.Keiluweit was supported by a Lawrence Scholar Fellowship awarded through Lawrence Livermore National Laboratory (LLNL). M.Kleber acknowledges support through Research Agreement No. 2014–1918 with the Institute of Soil Landscape Research, Leibniz-Center for Agricultural Landscape Research (ZALF), Müncheberg, Germany. This work was performed under the auspices of the US Department of Energy by LLNL under Contract DE-AC52-07NA27344. Funding was provided by LLNL LDRD 'Microbes and Minerals: Imaging C Stabilization' and a US DOE Genomics Science program award SA-DOE-29318 to J.P-R. The work of P.S.N. is supported by LBNL award No. IC006762 as sub-award from LLNL and DOE-BER Sustainable Systems SFA. The Advanced Light Source is supported by the Director, Office of Science, Office of Basic Energy Sciences, of the US DOE under Contract No. DE-AC02-05CH11231.

Author information

Affiliations

Department of Crop and Soil Science, Oregon State University, ALS Building 3017, Corvallis, Oregon 97331, USA

Marco Keiluweit & Markus Kleber

Chemical Sciences Division, Lawrence Livermore National Laboratory, 7000 East avenue, L-231, Livermore, California 94550, USA

Marco Keiluweit, Jeremy J. Bougoure, Jennifer Pett-Ridge & Peter K. Weber

School of Earth and Environment, University of Western Australia, 35 Stirling Highway, Crawley, Western Australia 6009, Australia

Jeremy J. Bougoure

Earth Sciences Division, Lawrence Berkeley National Laboratory, 1 Cyclotron Rd, Berkeley, California 94720, USA

Peter S. Nico

Institut für Bodenlandschaftsforschung, Leibnitz-Zentrum für Agrarlandschaftsforschung (ZALF) e.V. Eberswalder Straße 84, 15374 Müncheberg, Germany

Markus Kleber

Contributions

M.Keiluweit performed microcosm set-up, laboratory analyses, synchrotron analyses, data analysis and wrote the manuscript. J.J.B. was responsible for DNA/RNA extractions and data processing. J.J.B. and P.K.W. conducted NanoSIMS analyses. M.Kleber., J.P-R., P.K.W. and P.S.N. supervised the project. All authors discussed the results and contributed to the manuscript.

Competing interests

The authors declare no competing financial interests.

References

1. Högberg, P. *et al.* Large-scale forest girdling shows that current photosynthesis drives soil respiration. *Nature* **411**, 789–792 (2001).
2. Clemmensen, K. E. *et al.* Roots and associated fungi drive long-term carbon sequestration in boreal forest. *Science* **339**, 1615–1618 (2013).
3. Phillips, R. P., Finzi, A. C. & Bernhardt, E. S. Enhanced root exudation induces microbial feedbacks to N cycling in a pine forest under long-term CO₂ fumigation. *Ecol. Lett.* **14**, 187–194 (2011).
4. Carney, K. M., Hungate, B. A., Drake, B. G. & Megonigal, J. P. Altered soil microbial community at elevated CO₂ leads to loss of soil carbon. *Proc. Natl Acad. Sci. USA* **104**, 4990–4995 (2007).
5. DeLucia, E. H., Callaway, R. M., Thomas, E. M. & Schlesinger, W. H. Mechanisms of phosphorus acquisition for ponderosa pine seedlings under high CO₂ and temperature. *Ann. Bot.* **79**, 111–120 (1997).
6. Fransson, P. Elevated CO₂ impacts ectomycorrhiza-mediated forest soil carbon flow: Fungal biomass production, respiration and exudation. *Fungal Ecol.* **5**, 85–98 (2012).
7. Heimann, M. & Reichstein, M. Terrestrial ecosystem carbon dynamics and climate feedbacks. *Nature* **451**, 289–292 (2008).

8. Kuzyakov, Y., Friedel, J. K. & Stahr, K. Review of mechanisms and quantification of priming effects. *Soil Biol. Biochem.* **32**, 1485–1498 (2000).
9. Bianchi, T. S. The role of terrestrially derived organic carbon in the coastal ocean: A changing paradigm and the priming effect. *Proc. Natl Acad. Sci. USA* **108**, 19473–19481 (2011).
10. Fontaine, S., Mariotti, A. & Abbadie, L. The priming effect of organic matter: A question of microbial competition? *Soil Biol. Biochem.* **35**, 837–843 (2003).
11. Horvath, R. S. Microbial co-metabolism and the degradation of organic compounds in nature. *Bacteriol. Rev.* **36**, 146–155 (1972).
12. Blagodatskaya, E. & Kuzyakov, Y. Mechanisms of real and apparent priming effects and their dependence on soil microbial biomass and community structure: Critical review. *Biol. Fertil. Soils* **45**, 115–131 (2008).
13. Torn, M. S., Trumbore, S. E., Chadwick, O. A., Vitousek, P. M. & Hendricks, D. M. Mineral control of soil organic carbon storage and turnover. *Nature* **389**, 170–173 (1997).
14. Baisden, W. T., Amundson, R., Cook, A. C. & Brenner, D. L. Turnover and storage of C and N in five density fractions from California annual grassland surface soils. *Glob. Biogeochem. Cycles* **16**, 1117 (2002).
15. Mikutta, R. *et al.* Biodegradation of forest floor organic matter bound to minerals via different binding mechanisms. *Geochim. Cosmochim. Acta* **71**, 2569–2590 (2007).
16. Chorover, J. & Amistadi, M. K. Reaction of forest floor organic matter at goethite, birnessite and smectite surfaces. *Geochim. Cosmochim. Acta* **65**, 95–109 (2001).
17. Conant, R. T. *et al.* Temperature and soil organic matter decomposition rates—synthesis of current knowledge and a way forward. *Glob. Change Biol.* **17**, 3392–3404 (2011).
18. Mikutta, R., Kleber, M., Torn, M. S. & Jahn, R. Stabilization of soil organic matter: Association with minerals or chemical recalcitrance? *Biogeochemistry* **77**, 25–56 (2006).
19. Rasmussen, C., Southard, R. J. & Horvath, W. R. Soil mineralogy affects conifer forest soil carbon source utilization and microbial priming. *Soil Sci. Soc. Am. J.* **71**, 1141–1150 (2007).
20. Kemmitt, S. J. *et al.* Mineralization of native soil organic matter is not regulated by the size, activity or composition of the soil microbial biomass—a new perspective. *Soil Biol. Biochem.* **40**, 61–73 (2008).
21. Schmidt, M. W. I. *et al.* Persistence of soil organic matter as an ecosystem property. *Nature* **478**, 49–56 (2011).

22. Tang, J. Y., Riley, W. J., Koven, C. D. & Subin, Z. M. CLM4-BeTR, a generic biogeochemical transport and reaction module for CLM4: Model development, evaluation, and application. *Geosci. Model Dev.* **6**, 127–140 (2013).
23. Jones, D. L., Dennis, P. G. & vanHees, P. A. W. Organic acid behavior in soils—misconceptions and knowledge gaps. *Plant Soil* **248**, 31–41 (2003).
24. Neumann, G. & Roemheld, V. *The Rhizosphere: Biochemistry and Organic Substances at the Soil-Plant Interface* (CRC Press, 2007).
25. Paterson, E. & Sim, A. Rhizodeposition and C-partitioning of *Lolium perenne* in axenic culture affected by nitrogen supply and defoliation. *Plant Soil* **216**, 155–164 (1999).
26. Phillips, R. P., Erlitz, Y., Bier, R. & Bernhardt, E. S. New approach for capturing soluble root exudates in forest soils. *Funct. Ecol.* **22**, 990–999 (2008).
27. Brant, J. B., Sulzman, E. W. & Myrold, D. D. Microbial community utilization of added carbon substrates in response to long-term carbon input manipulation. *Soil Biol. Biochem.* **38**, 2219–2232 (2006).
28. Frey, S. D., Lee, J., Melillo, J. M. & Six, J. The temperature response of soil microbial efficiency and its feedback to climate. *Nature Clim. Change* **3**, 395–398 (2013).
29. Schneckenberger, K., Demin, D., Stahr, K. & Kuzyakov, Y. Microbial utilization and mineralization of [¹⁴C]glucose added in six orders of concentration to soil. *Soil Biol. Biochem.* **40**, 1981–1988 (2008).
30. Fierer, N., Bradford, M. A. & Jackson, R. B. Toward an ecological classification of soil bacteria. *Ecology* **88**, 1354–1364 (2007).
31. Eilers, K. G., Debenport, S., Anderson, S. & Fierer, N. Digging deeper to find unique microbial communities: The strong effect of depth on the structure of bacterial and archaeal communities in soil. *Soil Biol. Biochem.* **50**, 58–65 (2012).
32. Yan, F., Schubert, S. & Mengel, K. Soil pH increase due to biological decarboxylation of organic anions. *Soil Biol. Biochem.* **28**, 617–624 (1996).
33. McBride, M. B. *Environmental Chemistry of Soils* (Oxford Univ. Press, 1994).
34. Lovley, D. R. Dissimilatory Fe(III) and Mn(IV) reduction. *Microbiol. Rev.* **55**, 259–287 (1991).
35. Glinski, J., Stahr, K., Stepniewska, Z. & Brzezinska, M. Changes of redox and pH conditions in a flooded soil amended with glucose and nitrate under laboratory conditions. *J. Plant Nutr. Soil Sci.* **155**, 13–17 (1992).

36. Hamer, U. & Marschner, B. Priming effects in different soil types induced by fructose, alanine, oxalic acid and catechol additions. *Soil Biol. Biochem.* **37**, 445–454 (2005).
37. Falchini, L., Naumova, N., Kuikman, P. J., Bloem, J. & Nannipieri, P. CO₂ evolution and denaturing gradient gel electrophoresis profiles of bacterial communities in soil following addition of low molecular weight substrates to simulate root exudation. *Soil Biol. Biochem.* **35**, 775–782 (2003).
38. Liu, S. Y. *et al.* Synchrotron-based mass spectrometry to investigate the molecular properties of mineral–organic associations. *Anal. Chem.* **85**, 6100–6106 (2013).
39. Hanley, L. & Zimmermann, R. Light and molecular ions: The emergence of vacuum UV single-photon ionization in MS. *Anal. Chem.* **81**, 4174–4182 (2009).
40. Fischer, H., Ingwersen, J. & Kuzyakov, Y. Microbial uptake of low-molecular-weight organic substances out-competes sorption in soil. *Eur. J. Soil Sci.* **61**, 504–513 (2010).
41. Mikutta, R. *et al.* Biogeochemistry of mineral–organic associations across a long-term mineralogical soil gradient (0.3–4100 kyr), Hawaiian Islands. *Geochim. Cosmochim. Acta* **73**, 2034–2060 (2009).
42. Kramer, M. G., Sanderman, J., Chadwick, O. A., Chorover, J. & Vitousek, P. M. Long-term carbon storage through retention of dissolved aromatic acids by reactive particles in soil. *Glob. Change Biol.* **18**, 2594–2605 (2012).
43. Kunhi Mouvenchery, Y., Kučerík, J., Diehl, D. & Schaumann, G. E. Cation-mediated cross-linking in natural organic matter: A review. *Rev. Environ. Sci. Biotechnol.* **11**, 41–54 (2011).
44. Fischer, W. R., Flessa, H. & Schaller, G. pH values and redox potentials in microsites of the rhizosphere. *Z. Für Pflanzenernähr. Bodenkd.* **152**, 191–195 (1989).
45. Collignon, C., Ranger, J. & Turpault, M. P. Seasonal dynamics of Al- and Fe-bearing secondary minerals in an acid forest soil: Influence of Norway spruce roots (*Picea abies* (L.) Karst.). *Eur. J. Soil Sci.* **63**, 592–602 (2012).
46. Richter, D. D., Markewitz, D., Trumbore, S. E. & Wells, C. G. Rapid accumulation and turnover of soil carbon in a re-establishing forest. *Nature* **400**, 56–58 (1999).
47. Wieder, W. R., Grandy, A. S., Kallenbach, C. M. & Bonan, G. B. Integrating microbial physiology and physio-chemical principles in soils with the Microbial-Mineral Carbon Stabilization (MIMICS) model. *Biogeosciences* **11**, 3899–3917 (2014).
48. Hodge, A. *et al.* Characterisation and microbial utilisation of exudate material from the rhizosphere of *Lolium perenne* grown under CO₂ enrichment. *Soil Biol. Biochem.* **30**, 1033–1043 (1998).

49. Cheng, L. *et al.* Atmospheric CO₂ enrichment facilitates cation release from soil. *Ecol. Lett.* **13**, 284–291 (2010).
50. Pérez, D. V., de Campos, R. C. & Novaes, H. B. Soil solution charge balance for defining the speed and time of centrifugation of two Brazilian soils. *Commun. Soil Sci. Plant Anal.* **33**, 2021–2036 (2002).
51. Kilcoyne, A. L. D. *et al.* Interferometer-controlled scanning transmission X-ray microscopes at the Advanced Light Source. *J. Synchrotron Radiat.* **10**, 125–136 (2003).
52. Smith, R. M. & Martell, A. E. Critical stability constants, enthalpies and entropies for the formation of metal complexes of aminopolycarboxylic acids and carboxylic acids. *Sci. Total Environ.* **64**, 125–147 (1987).
53. Højberg, O. & Sørensen, J. Microgradients of microbial oxygen consumption in a barley rhizosphere model system. *Appl. Environ. Microbiol.* **59**, 431–437 (1993).